An Equation-of-State Contribution for Polar Components: Dipolar Molecules

Joachim Gross
Chair for Separation Technology, Delft University of Technology, 2628 CA Delft, The Netherlands

Jadran Vrabec
Institut für Technische Thermodynamik und Thermische Verfahrenstechnik, Universität Stuttgart, 70550 Stuttgart, Germany

DOI 10.1002/aic.10683
Published online October 6, 2005 in Wiley InterScience (www.interscience.wiley.com).

Accounting for dipolar interactions in a physically based equation of state (EOS) can substantially improve the modeling of phase equilibria of real mixtures. An EOS contribution for dipolar interactions of nonspherical molecules is developed based on a third-order perturbation theory. Molecular simulation data for vapor–liquid equilibria of the two-center Lennard–Jones (2CLJ) plus pointdipole fluid is used to determine model constants of the EOS. The resulting model is compared to simulation data of pure dipolar nonspherical molecules and their mixtures and an excellent agreement is found. The proposed dipole term is applied to real substances with the perturbed-chain statistical associating fluid theory (PC-SAFT) EOS and it is confirmed that accounting for dipolar interactions not only reduces the binary interaction parameter, but also improves the description of pure component and mixture phase equilibria. Literature values for the dipole moment can thereby be used and no further dipole-related pure component parameter has to be adjusted. This constitutes an advantage over earlier approaches, where dipole-related parameters were fitted to pure component data or to mixture data.
© 2005 American Institute of Chemical Engineers *AIChE J,* 52: 1194–1204, 2006

Introduction

Many of the newer thermodynamic models applied in science and engineering practice are derived from statistical mechanical fluid theories. The description of long-range interactions, whether from polar charge distribution or from permanent (ionic) charges, however, remains challenging. Although appropriate theories are available for dilute conditions, the behavior of dense polar or ionic fluids is subject to extensive research. Molecular simulations have long since played an important role in evaluating fluid theories but they may also more directly aid in bridging the gap to polar systems, as a previous investigation—among many other examples—targeting on quadrupolar molecules has shown.[1]

There are two prominent routes toward a description of dipolar interactions. One is given through integral equations and the other is through perturbation theories, where a known nonpolar reference fluid is defined and the dipolar contribution to the intermolecular interactions is considered as a perturbation. Perturbation theories for polar fluids converge slowly and are thus commonly given as third-order expansions written in a Padé approximation, as first suggested by Stell et al.[2,3] Simple engineering-like expressions for the involved pair correlation integrals were proposed by Rushbrooke et al.[4] for fluids exhibiting hard repulsion and later, also accounting for ionic charges, by Henderson et al.[5] Gubbins and Twu[6] elaborated multipolar and nonspherical components, and their mixtures, and derived simple expressions for fluids with a Lennard–Jones (LJ) reference potential. Those equation-of-state (EOS) contributions

Correspondence concerning this article should be addressed to J. Gross at J.Gross@wbmt.tudelft.nl.

© 2005 American Institute of Chemical Engineers

were subsequently applied to real substances in combination with different equations of state.[7-10] Later, several modifications of the *statistical associating fluid theory* (SAFT) EOS developed by Chapman et al.,[11] based on the thermodynamic perturbation theory of first order,[12-15] were applied to polar fluids. Kraska and Gubbins[16] thereby considered LJ-chain molecules, whereas Jog and Chapman[17] developed an expression suitable for multiple polar sites in chain molecules. The *perturbed-chain statistical associating fluid theory* (PC-SAFT) EOS of Gross and Sadowski[18,19] was applied to quadrupolar substances[20] considering a quadrupole term proposed by Saager and Fischer.[21] Excellent results were also obtained by Tumakaka and Sadowski[22] using the approach of Jog and Chapman for copolymers. The effect of nonspherical molecular shape on the polar contribution was studied by Boublik[23,24] considering the radial distribution function of a Gaussian overlap fluid. A far-reaching investigation on the structure and vapor–liquid equilibria of dipolar site–site fluids was presented by Lupkowski and Monson[25,26] and McGuigan et al.[27] Their work is based on cluster perturbation theory and delivers remarkable results when compared to simulation data, as a study by Dubey et al.[28] shows.

Molecular simulation data for structural properties (pair-correlation function) of the reference fluid has gone into most of the aforementioned models, whereas Saager et al.[29] and Saager and Fischer[21] have suggested a different approach. Rather than using structural (microscopic) properties from molecular simulations, they performed molecular simulations for vapor–liquid equilibria and used properties of the macroscopic system to obtain a dipole–dipole term and a quadrupole–quadrupole term by fitting empirical expressions to the simulation data. The simulations were performed for two-center Lennard–Jones (2CLJ) plus pointdipole fluids with fixed molecular elongation ($L^* = 0.505$). This approach was shown to give good results for real substances,[30-32] whereas the application to strongly asymmetric mixtures is nontrivial because of the empirical nature of the polar expressions.

In this work, an equation-of-state contribution for dipolar interactions of nonspherical molecules is derived. The model is based on a third-order perturbation theory written in the Padé approximation and model constants were adjusted to comprehensive vapor–liquid equilibrium data[33] of pure 2CLJ plus pointdipole molecules. The advantage of adopting the mathematical form of a perturbation theory is on the one hand the obvious treatment of mixtures and on the other hand the simple extension to strongly nonspherical components and asymmetric mixtures. After an outline of the theory and a comparison of the EOS to molecular simulation data, the dipole term in combination with the PC-SAFT EOS is applied to real substances.

Theory

Our interest focused on deriving a model suitable for polar and strongly nonspherical (chain) molecules and we thus eventually aim at an EOS contribution for tangent-sphere chain models. The tangent-sphere model assumes molecules to consist of chains of m freely jointed spherical segments, where, for the case of a noninteger value for m, the model is not rigorously defined. It was shown previously,[1] however, that for small molecules with segment numbers ($1 \leq m \leq 2$), the tangent-sphere model can with good precision be brought to congruence with the more elaborate 2CLJ model. This is important here because it allows the development of an EOS suited for both molecular models.

The 2CLJ plus pointdipole model consists of two Lennard–Jones sites located at a distance L apart from each other and a pointdipolar site of moment μ positioned in the geometric center and aligned along the molecular axis. The intermolecular pair potential can thereby be divided into that of a 2CLJ fluid and the contribution from the dipolar forces, as

$$u(\mathbf{r}_{ij}, \boldsymbol{\omega}_i, \boldsymbol{\omega}_j) = u^{2CLJ}(\mathbf{r}_{ij}, \boldsymbol{\omega}_i, \boldsymbol{\omega}_j) + u^{DD}(\mathbf{r}_{ij}, \boldsymbol{\omega}_i, \boldsymbol{\omega}_j) \quad (1)$$

where $\mathbf{r}_{ij}$ is the vector from one molecular center to the other and $\boldsymbol{\omega}_i$ denotes a set of two molecular orientation angles $\{\theta_i, \phi_i\}$. The pair potential of the pure 2CLJ fluid can conveniently be written as a two-site LJ potential

$$u^{2CLJ}(\mathbf{r}_{ij}, \boldsymbol{\omega}_i, \boldsymbol{\omega}_j) = \sum_{\alpha=1}^{2} \sum_{\beta=1}^{2} 4\varepsilon \left[\left(\frac{\sigma}{r_{\alpha\beta}} \right)^{12} - \left(\frac{\sigma}{r_{\alpha\beta}} \right)^{6} \right] \quad (2)$$

where σ and ε are, respectively, the Lennard–Jones segment size and segment energy parameters; and $r_{\alpha\beta}$ is the distance between two LJ sites of different molecules i and j. The dipolar contribution[34] is

$$u^{DD}(\mathbf{r}_{ij}, \boldsymbol{\omega}_i, \boldsymbol{\omega}_j) = -\mu_i \mu_j |\mathbf{r}_{ij}|^{-3} \times [2 \cos\theta_i \cos\theta_j - \sin\theta_i \sin\theta_j \cos(\phi_j - \phi_i)] \quad (3)$$

where μ_i is the dipole moment, θ_i is the polar angle of the dipole formed with the vector $\mathbf{r}_{ij}$, and ϕ_i is the azimuthal angle thereof.

By applying a perturbation theory to the intermolecular potential, Eq. 1 results in an EOS given in the residual Helmholtz energy A^{res}, as

$$\frac{A^{res}}{NkT} = \frac{A^{2CLJ}}{NkT} + \frac{A^{DD}}{NkT} \quad (4)$$

where A^{2CLJ} is the residual Helmholtz energy of the 2CLJ reference fluid, A^{DD} is the contribution from dipole–dipole interactions, N denotes the total number of molecules, and k is the Boltzmann constant.

Similar to our previous work,[1] we consider an EOS for A^{2CLJ} in Eq. 4, which is based on the thermodynamic perturbation theory of first order[11-15] and consists of a Lennard–Jones EOS[35] and an expression for the radial distribution function $g^{LJ}(\sigma)$ in the so-called chain term.[36]

Here it is necessary to translate between the molecular parameters of the tangent-sphere model and the 2CLJ model and, to do so, we adopt a simple scheme, where the segment size parameter σ for both models is equal and thus

$$\sigma = \sigma^{2CLJ} \qquad \varepsilon = \frac{4}{m^2}\varepsilon^{2CLJ} \qquad \mu^{*2} = \frac{m}{4}(\mu^{*2CLJ})^2$$
$$T^* = \frac{m^2}{4} T^{*2CLJ} \qquad P^* = \frac{m^3}{4} P^{*2CLJ} \quad (5)$$

Table 1. Model Constants of the Dipole Equation-of-State Contribution

i	a_{0i}	a_{1i}	a_{2i}	b_{0i}	b_{1i}	b_{2i}	c_{0i}	c_{1i}	c_{2i}
0	0.3043504	0.9534641	−1.1610080	0.2187939	−0.5873164	3.4869576	−0.0646774	−0.9520876	−0.6260979
1	−0.1358588	−1.8396383	4.5258607	−1.1896431	1.2489132	−14.915974	0.1975882	2.9924258	1.2924686
2	1.4493329	2.0131180	0.9751222	1.1626889	−0.5085280	15.372022	−0.8087562	−2.3802636	1.6542783
3	0.3556977	−7.3724958	−12.281038	0	0	0	0.6902849	−0.2701261	−3.4396744
4	−2.0653308	8.2374135	5.9397575	0	0	0	0	0	0

Every dimensionless molecular elongation $L^* = L/\sigma$ is then (with satisfactory precision) related to an equivalent segment number m and this dependency was determined by adjusting m to simulation data of the 2CLJ fluid from Stoll et al.[33] The relation between elongation L^* and segment number m is then given by

$$m = 1 + 0.1795L^* + 3.3283L^{*2} - 3.8855L^{*3} + 1.3777L^{*4} \qquad \text{for } 0 \le L^* \le 1 \quad (6)$$

This expression is slightly different from the one obtained earlier[1] because the simulation data for the nonpolar 2CLJ fluid were somewhat improved in the work of Stoll et al.[33] compared with earlier data from the same group.[37]

In the perturbation theory we consider terms of up to third order written in the Padé approximation,[3] so that the Helmholtz energy contribution A^{DD} to Eq. 4 is given as

$$\frac{A^{DD}}{NkT} = \frac{A_2/NkT}{1 - A_3/A_2} \quad (7)$$

with A_2 and A_3 as the second-order and third-order perturbation terms, respectively. For linear and symmetric molecules, these perturbation terms can be written[1,24,34] as

$$\frac{A_2}{NkT} = -\pi\rho \sum_i \sum_j x_i x_j \frac{\varepsilon_{ii}}{kT}\frac{\varepsilon_{jj}}{kT}\frac{\sigma_{ii}^3\sigma_{jj}^3}{\sigma_{ij}^3} n_{\mu,i} n_{\mu,j} \mu_i^{*2}\mu_j^{*2} J_{2,ij}^{DD} \quad (8)$$

and

$$\frac{A_3}{NkT} = -\frac{4\pi^2}{3}\rho^2 \sum_i \sum_j \sum_k \times x_i x_j x_k \frac{\varepsilon_{ii}}{kT}\frac{\varepsilon_{jj}}{kT}\frac{\varepsilon_{kk}}{kT}\frac{\sigma_{ii}^3\sigma_{jj}^3\sigma_{kk}^3}{\sigma_{ij}\sigma_{ik}\sigma_{jk}} n_{\mu,i} n_{\mu,j} n_{\mu,k} \mu_i^{*2}\mu_j^{*2}\mu_k^{*2} J_{3,ijk}^{DD} \quad (9)$$

where ρ denotes the molecular number density, x_i is the mole fraction, $\mu_i^{*2} = \mu_i^2/(m_i\varepsilon_{ii}\sigma_{ii}^3)$ is the dimensionless squared dipole moment, and the combining rules are $\varepsilon_{ij} = (\varepsilon_i\varepsilon_j)^{0.5}$ and $\sigma_{ij} = (\sigma_i + \sigma_j)/2$. The abbreviations $J_{2,ij}$ and $J_{3,ijk}$ denote integrals over the reference-fluid pair-correlation function and over three-body correlation functions, respectively. With the same reasoning as in a previous study[1] we assume simple power functions for these integrals, as

$$J_{2,ij}^{DD} = \sum_{n=0}^{4} \left(a_{n,ij} + b_{n,ij}\frac{\varepsilon_{ij}}{kT}\right)\eta^n \quad (10)$$

$$J_{3,ijk}^{DD} = \sum_{n=0}^{4} c_{n,ijk}\eta^n \quad (11)$$

where η is a dimensionless density and the relation between η and ρ depends on the considered EOS, as detailed in the appendix published in the work of Gross.[1] The coefficients in Eqs. 10 and 11 depend on chain length m with

$$a_{n,ij} = a_{0n} + \frac{m_{ij}-1}{m_{ij}}a_{1n} + \frac{m_{ij}-1}{m_{ij}}\frac{m_{ij}-2}{m_{ij}}a_{2n} \quad (12)$$

$$b_{n,ij} = b_{0n} + \frac{m_{ij}-1}{m_{ij}}b_{1n} + \frac{m_{ij}-1}{m_{ij}}\frac{m_{ij}-2}{m_{ij}}b_{2n} \quad (13)$$

and

$$c_{n,ijk} = c_{0n} + \frac{m_{ijk}-1}{m_{ijk}}c_{1n} + \frac{m_{ijk}-1}{m_{ijk}}\frac{m_{ijk}-2}{m_{ijk}}c_{2n} \quad (14)$$

and where for combining rules of the chain length, we define

$$m_{ij} = (m_i m_j)^{1/2} \qquad \text{with } m_{ij} \le 2 \quad (15)$$

$$m_{ijk} = (m_i m_j m_k)^{1/3} \qquad \text{with } m_{ijk} \le 2 \quad (16)$$

The model constants in Eqs. 12–14 were adjusted to simulation data of Stoll et al.,[33] whereby molecular simulations of the spherical Stockmayer fluids were considered for determining the 15 constants a_{0n}, b_{0n}, and c_{0n} and simulation data of nonspherical molecules, ranging from $L^* = 0.2$ to $L^* = 1$, were used to adjust the 21 selected constants a_{1n}, a_{2n}; b_{1n}, b_{2n}; and c_{1n}, c_{2n}. More specifically, the data considered for the fitting procedure consisted of vapor pressure data, saturated liquid and vapor density data ($0.55T^{*c} \le T^* \le 0.99T^{*c}$), and virial coefficients. The resulting model constants are given in Table 1.

An important restriction to the formalism suggested here is that the dipole moment is allowed to stretch over only two segments [that is, $m_{ij} \le 2$ and $m_{ijk} \le 2$ in Eqs. 15 and 16 because only molecules with an elongation of $L^* = 1$ (equivalent to $m = 2$) were considered in the regression of the model constants]. This restriction however does not imply that the molecules are restricted to two segments. Rather, it is possible

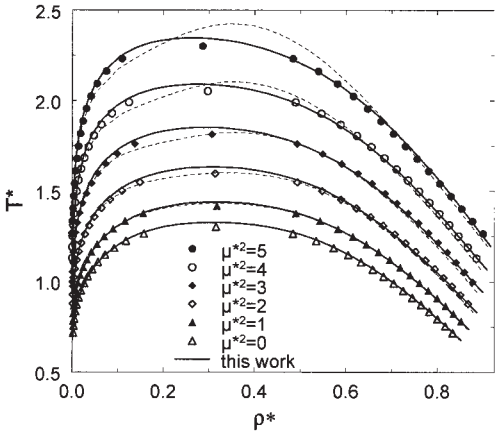

Figure 1. Vapor–liquid equilibrium of the spherical dipolar LJ fluid (Stockmayer fluid) for various squared dipole moments.

Comparison of simulation data (symbols: Stoll et al.[33]) to the proposed equation of state (EOS) theory (solid lines) and to the model of Saager and Fischer (dashed lines).

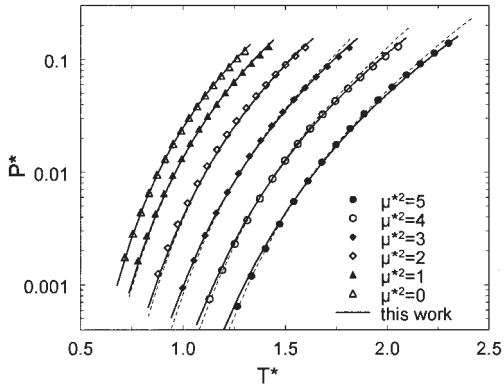

Figure 2. Vapor–pressure curves of the spherical dipolar LJ fluid (Stockmayer fluid) for various squared dipole moments.

Comparison of simulation data (symbols: Stoll et al.[33]) to the proposed EOS theory (solid lines) and to the model of Saager and Fischer (dashed lines).

to consider a molecule with larger segment number m, where the dipole moment (of a functional group) stretches over only two or fewer segments. This is ensured by limiting the values of m_{ij} and m_{ijk} to a maximum value of 2 in Eqs. 15 and 16 and the restriction thus acts only on the polar terms. If a molecule possesses multiple functional groups, such as copolymers with polar repeat units, then the number of dipolar moments per molecule is accounted for through the number of dipolar moments $n_{\mu,i}$ as suggested by Jog and Chapman[17,38] and in a somewhat different scheme by Walsh et al.[39] In the case of low molecular weight substances and within the scope of this study the number of dipolar moments $n_{\mu,i}$ is equal to unity.

A further restriction has gone into the model through the considered dipolar components, that is, the axial alignment of the dipole moment. It was shown by Vega et al.[40] that an orientation of dipole moments perpendicular to the molecular axis leads to a considerably more substantial effect on physical properties compared with the axial alignment. If the proposed EOS is applied to a component where the dipole vector is oriented, say perpendicular to the molecular axis, one can thus expect a dipolar contribution that is somewhat too low. Although in the present study we use only dipole moments from the literature to demonstrate the physical basis of the EOS, in the future it may also be a sensible measure to adjust a dipole-related parameter to pure component data.

Results for Pure 2CLJ Plus Dipole Fluids

A comparison of the proposed EOS with simulation data[33] for the vapor–liquid equilibrium of spherical LJ fluids (Stockmayer) with varying dipolar moments is given in Figures 1 and 2. A similar comparison is presented in Figures 3 and 4 for the case of different 2CLJ plus dipole fluids with an elongation of $L^* = 1$. Considering the wide range of conditions covered by the simulation data, the correlation results are highly satisfactory. The overestimation of the critical point is already observed for the nonpolar case and the polar contribution does not aggravate these deviations.

The model constants were adjusted to simulation data, al-

whereby Joule–Thomson inversion points were not considered. A comparison of Joule–Thomson inversion points[41] determined from molecular dynamics simulations and calculations of the EOS model are depicted in Figure 5. The diagrams indicate that the significant influence of a dipolar moment on this property is very well captured by the model.

Results for Mixtures of 2CLJ Plus Dipole Fluids

The vapor–liquid equilibria of a dipolar 2CLJ fluid and a nonpolar spherical LJ fluid are given in Figure 6. The simulation data of Stoll et al.[42] were generated for a mixture of real components (carbon monoxide and methane), considering a binary interaction parameter, and the phase behavior of the real mixture was reproduced with good accuracy. The binary interaction parameter considered in the molecular simulations was introduced to derive an improved representation of the behavior of the real mixture, which is defined as a correction to the unlike energy parameter of the Berthelot–Lorentz combining rule, as $\varepsilon_{ij} = (\varepsilon_i\varepsilon_j)^{0.5}(1 - k_{ij})$. This definition is also common

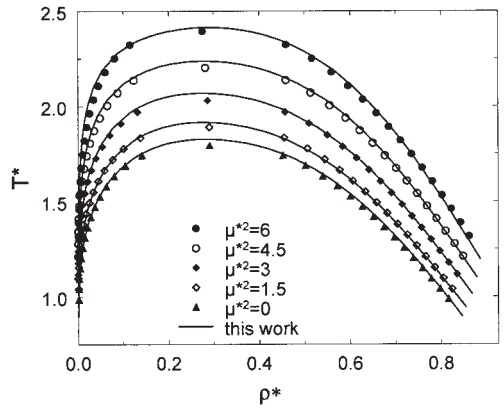

Figure 3. Vapor–liquid equilibrium of the 2CLJ fluid with fixed molecular elongation $L^* = 1$ (dimer) and various squared pointdipole moments μ^{*2}.

Comparison of simulation data (symbols: Stoll et al. [33]) to the proposed EOS theory (lines).

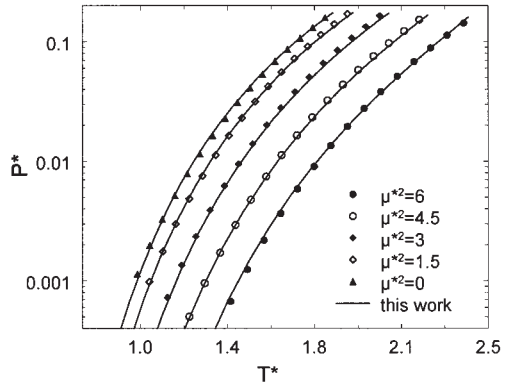

Figure 4. Vapor–pressure curves of the 2CLJ fluid with fixed molecular elongation $L^* = 1$ (dimer) and various squared pointdipole moments μ^{*2}.

Comparison of simulation data (symbols: Stoll et al.[33]) to the proposed EOS theory (lines).

in equations of state and the k_{ij} value introduced in the simulations can also be used in the theory. The EOS is thus applied without any adjustable parameter because the pure component parameters and the binary interaction correction considered in the simulations were used and, in doing so, the model is in

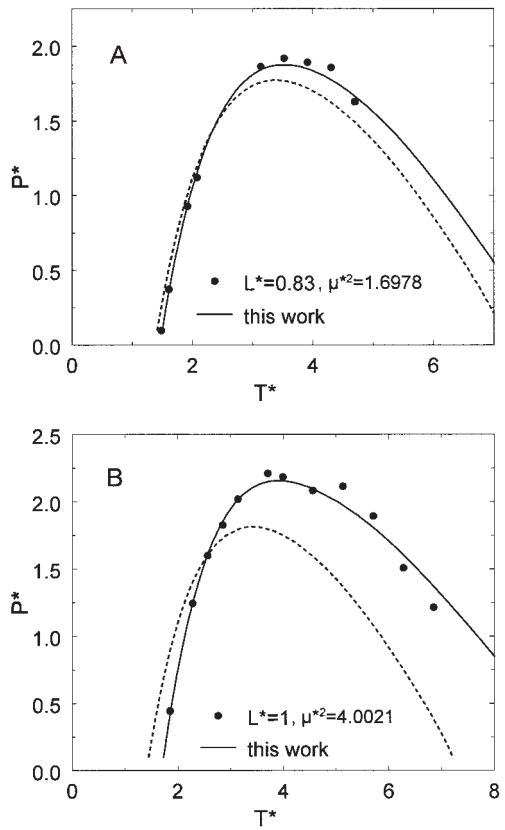

Figure 5. Joule–Thomson inversion points of the 2CLJ plus dipole fluid.

Molecular elongation L^* and dipole moments μ^{*2} as labeled in diagrams. Comparison of simulation data (symbols: Vrabec et al.[41]) to predictions of the proposed EOS theory (lines). Nonpolar 2CLJ (dotted line) considered for orientation.

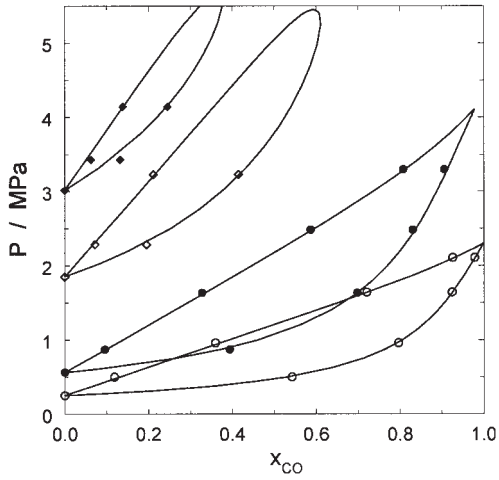

Figure 6. Simulation data (Stoll[42]) for the vapor–liquid equilibrium of a mixture of the 2CLJD [$L^* = 0.3455$ and $(\mu^{*2CLJ})^2 = 2.9710$] and the LJ fluid at four temperatures.

For the simulations, pure component parameters and binary interaction parameter were adjusted to describe a mixture of methane and carbon monoxide. Model prediction (no adjustable parameter) of the EOS (lines) using the same pure component and mixture parameters as in simulation.

good agreement with the simulated data. This is an important test for the dipole term because no mixing scheme of polar contributions is applied and the results solely reflect the functional form of the second- and third-order terms of the perturbation theory and their interplay in the Padé approximation. The vapor–liquid equilibrium of a mixture of two dipolar LJ (Stockmayer) fluids[43] is displayed in Figure 7 and the model is found to be in good agreement with the simulation data.

Liquid–liquid equilibria often mark a challenging and sensitive test for equations of state. De Leeuw et al.[44] conducted

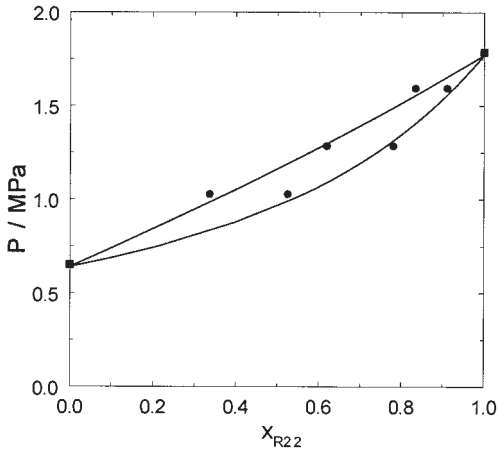

Figure 7. Simulation data (Gao et al.[43]) for the vapor–liquid equilibrium of a mixture of two spherical dipolar LJ (Stockmayer) molecules.

For the simulations, pure component parameters and binary interaction parameter were adjusted to describe a mixture of R142b and R22. Model prediction (no adjustable parameter) of the EOS (lines) using the same pure component and mixture parameters as in simulation.

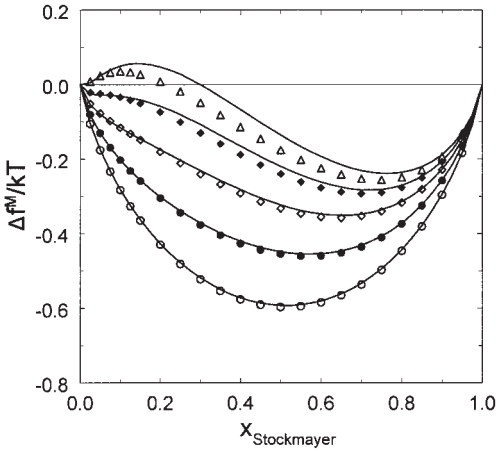

Figure 8. Helmholtz energy of mixing of Lennard–Jones–Stockmayer mixtures at $T^* = 1.15$ and $\rho^* = 0.822$ for five dipole moments of the Stockmayer fluids ($\mu^{*2} = \{1, 2, 3, 4, 5\}$ in order of increasing Helmholtz energy).

Comparison of simulation data (symbols: de Leeuw et al.[44]) and predictions of the proposed EOS (lines).

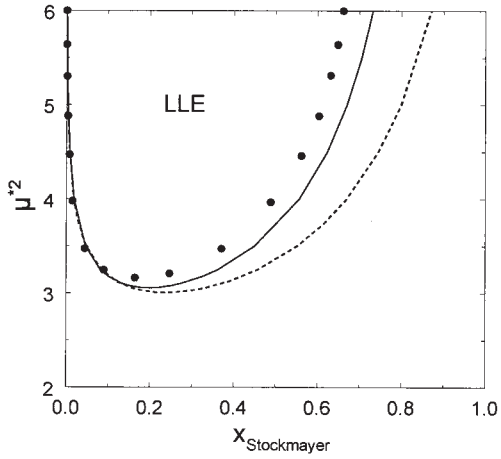

Figure 9. Liquid–liquid equilibria of Lennard–Jones–Stockmayer mixtures at $T^* = 1.15$.

The symbols are from simulation data (symbols: de Leeuw et al.[44]) for two (hypothetical) phases with fixed densities of $\rho^* = 0.822$. Solid line is the prediction of the proposed EOS using the same density in both phases. A prediction of the true liquid–liquid equilibrium according to the EOS at $P^* = 1$ is shown for comparison (dashed line).

molecular simulations to study the excess properties of mixtures with a dipolar component. To isolate the effect of varying dipole moments on the mixture behavior, they considered mixtures of Stockmayer and LJ fluids where both molecules possess identical LJ parameters. The Helmholtz energy of mixing is displayed in Figure 8 for a fixed temperature $T^* = 1.15$ and a typical liquid density ($\rho^* = 0.822$) and it becomes apparent from the shape of the curves that, for higher dipole moments, a liquid–liquid separation will occur. The proposed EOS is in good agreement with the simulation data. By constructing the excess Gibbs enthalpy of mixing, de Leeuw et al.[44] found that Stockmayer fluids with dipole moments above $\mu^{*2} = 3.15$ exhibit a liquid–liquid demixing with the LJ fluid at the specified conditions. Moreover, they derived a quasi-phase equilibrium diagram by assuming fixed densities in both phases, as depicted in Figure 9. The equivalent assumptions were introduced into the EOS by fixing the densities of the hypothetical phases to the value considered in the simulation. There is thus no adjustable parameter involved and the predictions of the EOS are in excellent agreement with the simulation data. A full and consistent liquid–liquid equilibrium calculation for a fixed pressure of $P^* = 1$ is also given in Figure 9 for comparison.

A similar study for the case of nonspherical molecules was carried out by Müller et al.[45] Figure 10 compares the Gibbs enthalpy of mixing as well as the excess contribution thereof as derived from simulation to the proposed EOS. Both the simulations and the model suggest complete miscibility for dipole moments of $(\mu^{*2CLJ})^2 = 4$ and 8, whereas a liquid–liquid demixing is found for a dipole moment of $(\mu^{*2CLJ})^2 = 12$.

Application to Real Components and Mixtures

The above-described model framework can be applied with the PC-SAFT EOS, as demonstrated earlier for quadrupolar components.[1] The derived dipole expressions can readily be incorporated by adding Eq. 7 to the appropriate equation of the Helmholtz energy in the PC-SAFT model.[19] For brevity, the EOS is referred to as *perturbed-chain polar SAFT* (PCP-SAFT). Throughout this study, we consider dipole moments as tabulated in the literature[46] and thus no additional parameter is introduced with the dipole term. Here we strive to demonstrate that accounting for dipole interactions will considerably improve correlation results for polar components and their mixtures. It is noteworthy, however, that a more comprehensive investigation will be presented in a subsequent study that also accounts for the polarizability of molecules and thus the induction of dipoles.

We determined the three pure component parameters of the

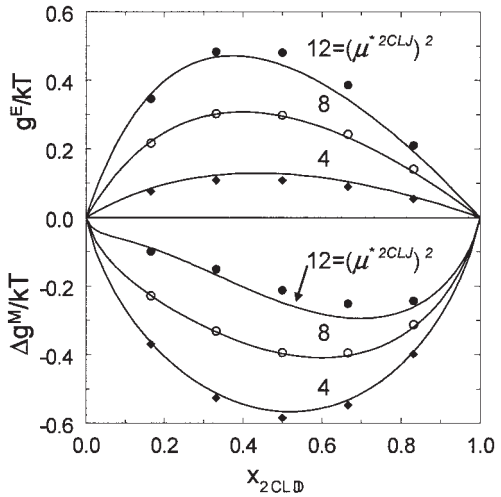

Figure 10. Gibbs enthalpy of mixing (bottom) and excess Gibbs enthalpy of mixing (top) for 2CLJ and 2CLJD mixtures at $T^{*2CLJ} = 2.1546$ and $P^* = 2.907$ with $L^* = 0.505$.

Comparison of simulation data (symbols: Müller et al.[45]) for three dipole moments of 2CLJD fluids and predictions of the proposed EOS (lines).

Table 2. PCP-SAFT Pure Component Parameters for Dipolar Components

Substance	M (g/mol)	m	σ (Å)	ε/k (K)	$\mu^{\dagger}$ (D)	AAD-% PCP-SAFT (AAD-% PC-SAFT) P^{sat}	ρ	Temp. Range (K)	Data Ref.[‡]
Ketones									
Acetone	58.08	2.7447	3.2742	232.99	2.88	0.55 (1.61)	1.31 (2.94)		1,2
Butanone	72.107	2.9835	3.4239	244.99	2.78	0.70 (1.52)	1.91 (2.82)		1,2
2-Pentanone	86.134	3.3537	3.4942	246.66	2.7	1.44 (1.87)	1.73 (1.83)		1,2
3-Pentanone	86.134	3.2786	3.5159	248.69	2.82	0.77 (0.85)	1.53 (2.02)		1,2
Aldehydes									
Propanal	58.08	2.6001	3.2872	235.21	2.72	0.75 (2.43)	0.77 (0.49)	193–503	1,2
Butanal	72.107	2.8825	3.4698	247.09	2.72	1.58 (1.53)	2.00 (2.57)	248–535	1,2
Esters									
Methyl methanoate	60.053	2.6225	3.1095	239.05	1.77	1.45 (1.17)	1.03 (1.48)	174–487	2
Ethyl methanoate	74.079	2.8338	3.3316	244.50	1.93	0.79 (0.92)	1.52 (1.80)	193–508	2
Propyl methanoate	88.106	3.1723	3.4296	245.64	1.89	0.90 (0.95)	0.87 (1.01)	270–538	2
Ethyl ethanoate	88.106	3.5060	3.3177	230.24	1.78	1.28 (1.30)	2.15 (2.24)	190–523	2
Propyl ethanoate	102.13	3.7658	3.4289	235.42	1.78	1.17 (1.22)	1.01 (1.07)	260–549	2
n-Butyl ethanoate	116.16	3.9629	3.5482	242.27	1.87	2.05 (2.03)	1.21 (1.26)	200–579	2
Methyl propanoate	88.106	3.4442	3.3255	234.26	1.85	1.18 (1.26)	1.76 (1.87)	186–530	2
Ethyl propanoate	102.133	3.7954	3.4169	233.09	1.74	1.20 (1.26)	1.16 (1.22)	240–546	2
Propyl propanoate	116.16	4.0993	3.4921	235.38	1.8	3.60 (3.53)	0.69 (0.75)	220–568	2
Methyl butanoate	102.133	3.6420	3.4535	240.02	2.03	1.04 (1.12)	0.88 (0.96)	240–554	2
Ethers									
Dimethyl ether	46.069	2.2634	3.2723	210.29	1.3	0.24 (0.25)	0.53 (0.80)	200–400	2,3
Methyl ethyl ether	60.096	2.6425	3.3794	215.79	1.17	1.94 (1.96)	0.45 (0.41)	270–437	2,3
Methyl *n*-propyl ether	74.123	3.0004	3.4602	222.67	1.107	1.97 (1.99)	1.07 (1.04)	220–476	2
Diethyl ether	74.123	2.9726	3.5127	219.53	1.15	0.66 (0.68)	1.01 (1.04)	220–466	2
Miscellaneous									
DMSO	78.13	3.0243	3.2427	309.36	3.96	0.46 (1.45)	0.33 (0.58)	291–519	1
HCl	36.461	1.5194	2.9794	203.32	1.109	0.80 (1.19)	0.73 (0.57)	150–324	2
Chloro methane	50.488	1.8070	3.3034	229.97	1.896	0.47 (0.60)	0.46 (1.71)	283–416	4
Chloro ethane	64.514	2.2207	3.4335	237.03	2.05	1.09 (1.63)	1.33 (1.77)	135–460	2
Average						1.23 (1.42)	1.05 (1.23)		

[†]Dipole moments ($1D = 3.33564 \times 10^{-30}$ cm) from the literature.[46] For dimensionless dipole moments from parameters in units as specified, it is $\mu_i^{*2} = \mu_i^2/(m_i\sigma_{ii}^3\varepsilon_{ii}/k) \times 10^4/1.3807\ \text{Å}^3 \times K/D^2$.

[‡]References: (1) Korea Thermophysical Properties Data Bank, http://www.cheric.org/kdb/, 2004; (2) Daubert TE, Danner RP, Sibul HM, Stebbins CC. *Physical and Thermodynamic Properties of Pure Chemicals: Data Compilation.* Washington, DC: Taylor & Francis, 1989; (3) *VDI-Wärmeatlas.* 7th Edition. Düsseldorf, Germany: VDI-Gesellschaft Verfahrenstechnik und Chemieingenieurwesen (GVC), 1994; (4) Hsu CC, McKetta JJ. Pressure–volume–temperature properties of methyl chloride. *J Chem Eng Data* 1964;9:45–51.

PCP-SAFT EOS for a number of polar components preferentially from triple point to critical point. Table 2 presents the pure component parameters and the correlation results in terms of the average absolute deviations (AADs) and, for comparison, the numbers in the parentheses are results of the nonpolar PC-SAFT EOS considering the same pure component data. It becomes apparent from the AAD values in Table 2 that the correlation results of components with high dipole moments are substantially improved, when dipolar interactions are taken into account, whereas for ethers as weak dipoles, of course, only slight improvement is found. Figure 11 shows the vapor–liquid equilibrium of acetone in a T–ρ diagram. The coexisting densities as calculated from PCP-SAFT are in good agreement with the experimental data, whereas considerable deviations are seen for the case where the dipole term is omitted (PC-SAFT). A clear improvement of the PCP-SAFT EOS is also found for the enthalpy of vaporization, as displayed in Figure 12.

The vapor–liquid equilibria of mixtures of acetone with nonpolar components of varying molecular elongation (ethane,[48] *n*-butane,[49] *n*-pentane,[50] decane[51]) are displayed in Figures 13 to 16, respectively. Accounting for the polar interactions reduces the (absolute) value of the binary interaction parameter and thus enhances the predictive capability of the model. More important, though, the description of the mixture behavior is improved. This is apparent for the liquid phase,

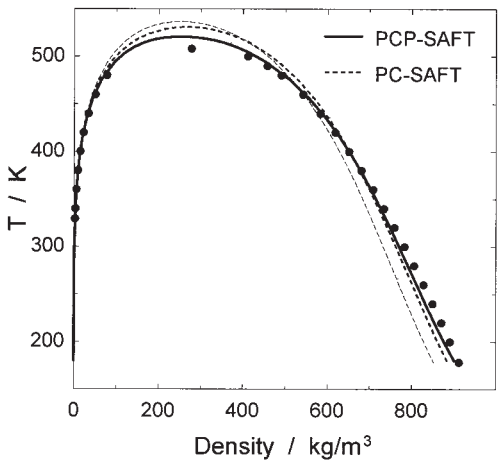

Figure 11. Saturated vapor and liquid densities of acetone.

Comparison of experimental data (symbols) to the PCP-SAFT EOS (solid lines) and the PC-SAFT model (short dashed lines). Results of the PC-SAFT EOS with the Jog–Chapman dipole term are given for comparison (thin dashed line).

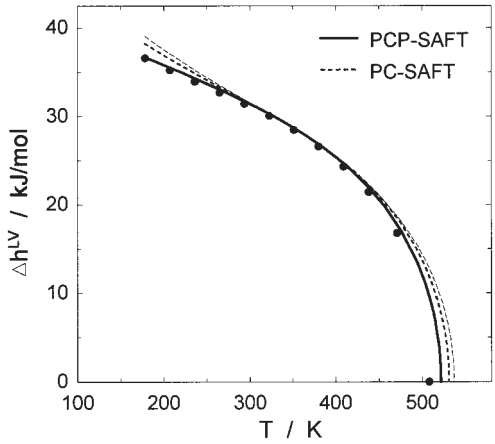

Figure 12. Enthalpy of vaporization of acetone.

Comparison of experimental data (symbols) to the PCP-SAFT EOS (solid lines) and the PC-SAFT model (short dashed lines). Results of the PC-SAFT EOS with the Jog–Chapman dipole term are given for comparison (thin dashed line).

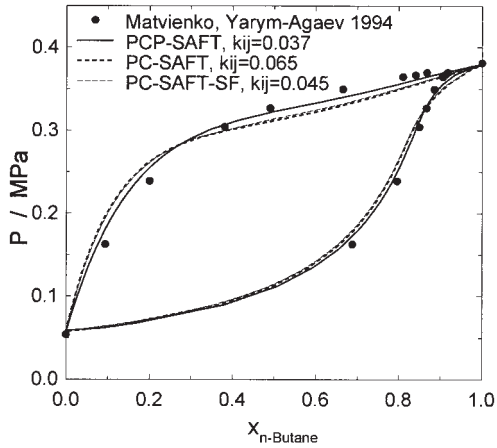

Figure 14. Vapor–liquid equilibrium of the acetone–*n*-butane mixture at $T = 40°C$.

Comparison of PCP-SAFT ($k_{ij} = 0.037$) and PC-SAFT ($k_{ij} = 0.066$) correlations to experimental data.[49]

where the solubility of nonpolar compounds in the acetone-rich phase is now in better agreement with experimental data. The enthalpy of mixing is an important indicator for the temperature behavior of thermodynamic models. Figure 17 gives the enthalpy of mixing for the acetone and *n*-decane system and the fair to good agreement of the PCP-SAFT model suggests robustness of the model toward extrapolations with temperature.

Finally, the vapor–liquid equilibrium of a dimethyl sulfoxide (DMSO) and toluene[52] system is shown in Figure 18. The improvement of the PCP-SAFT EOS as opposed to its nonpolar equivalent is very pronounced in this case as a result of the high dipolar moment of $\mu_i = 3.96D$ for DMSO.

The previously considered polar substances possess only single polar sites. For multifunctional molecules, the definition of a dipole moment is less unambiguous and we see two promising strategies for applying fluid theories to such components. On the one hand, and most obvious, one can adopt a group-contribution philosophy and assign dipolar moments to functional groups, adjusting either μ_i or $n_{\mu,i}$ to account for their effectiveness. Another appealing concept was proposed by Jin and Sandler,[53] who determined partial charges and dipolar moments of functional groups from quantum mechanical calculations. This procedure has the elegant advantage that the cancellation or aggravation of polar moments within a molecule can be accounted for.

Comparison to Existing Dipole Expressions

From several dipole theories for nonspherical molecules, the approaches of Jog and Chapman[17,22,38] and of Saager and Fischer[21] were elaborated in most detail and a comparison to these theories constitutes a meaningful test to the proposed PCP-SAFT EOS. The dipole expression of Jog and Chapman requires an adjustable dipole parameter when applied to real systems, that is, the effective fraction of dipolar sites per

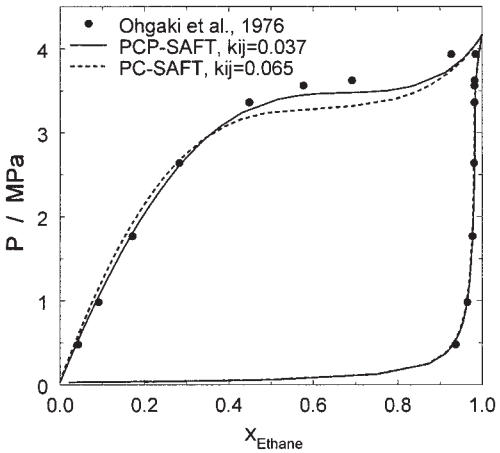

Figure 13. Vapor–liquid equilibrium of the acetone–ethane mixture at $T = 25°C$.

Comparison of PCP-SAFT ($k_{ij} = 0.037$) and PC-SAFT ($k_{ij} = 0.065$) correlations to experimental data.[48]

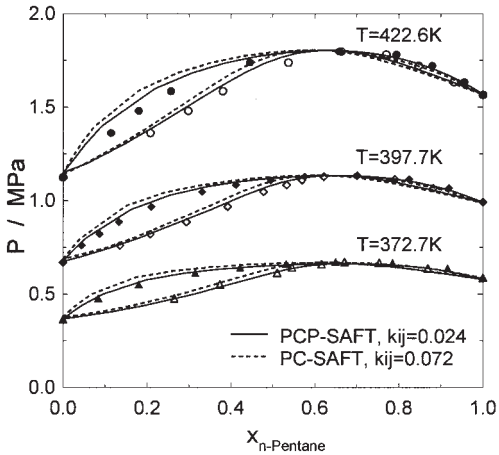

Figure 15. Vapor–liquid equilibrium of the acetone–*n*-pentane mixture at three temperatures.

Comparison of PCP-SAFT ($k_{ij} = 0.024$) and PC-SAFT ($k_{ij} = 0.072$) correlations to experimental data.[50]

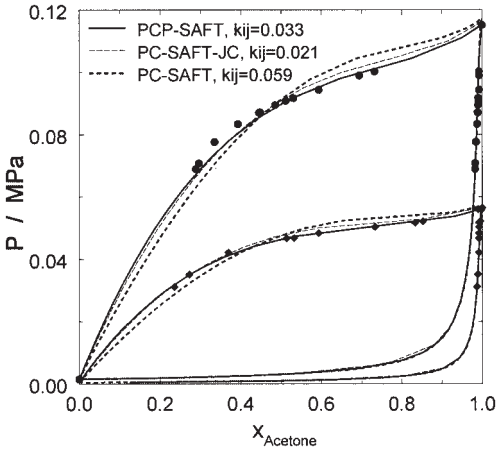

Figure 16. Vapor–liquid equilibrium of the acetone–*n*-decane mixture at $T = 60°C$ (spheres) and $T = 40°C$ (diamonds).

Comparison of PCP-SAFT, PC-SAFT, and PC-SAFT-Jog–Chapman correlations to experimental data.[51]

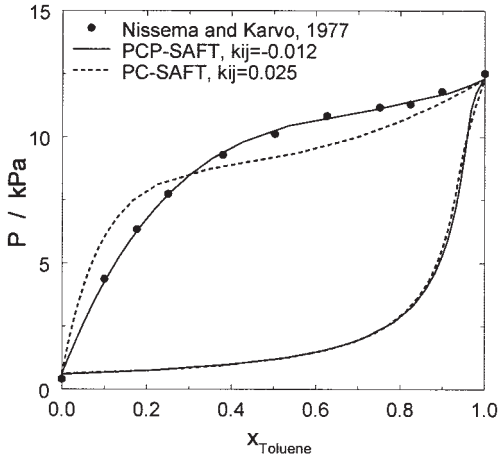

Figure 18. Vapor–liquid equilibrium for the dimethyl sulfoxide (DMSO)–toluene mixture at $T = 50°C$.

Comparison of PCP-SAFT and PC-SAFT correlations to experimental data.[52]

molecule $x_{p,i}$. For small molecules $x_{p,i}$ should ideally be $x_{p,i} = 1/m_i$. If this is assumed for the case of acetone to compare the Jog–Chapman term (PC-SAFT-JC) EOS to the PCP-SAFT model without adjusting dipole-related parameters, one finds a tendency of PC-SAFT-JC to predict wide liquid–liquid demixing behavior to all of the systems considered here. This malbehavior cannot be suppressed. If on the other hand either the dipole moment or the $x_{p,i}$ parameter of the PC-SAFT-JC model is adjusted to pure component data, the best fit is obtained when these parameters are zero and the dipole term vanishes. It may be added that this problem also persists when a Lennard–Jones reference[6] is considered, rather than the hard-sphere reference of Rushbrook et al.[4] Alternatively, it was suggested[22,38,54] to use binary mixture data along with pure component properties for fitting pure component parameters of the PC-SAFT-JC model and we use the resulting parameters proposed by Dominik et al.[54] The long-dashed lines in Figures 11 and 12 give the coexisting densities and the enthalpy of vaporization of pure acetone, respectively, and these diagrams show an advantage of the PCP-SAFT model for pure components. The phase equilibria of the mixtures considered herein are generally very well described by the PC-SAFT-JC EOS. A representative comparison is given in Figures 16 and 17. However, because mixture data were used in the regression of the pure component parameters of acetone, the comparison is not quite on equal ground and one can conclude it to be a considerable advantage of the PCP-SAFT model that no binary-mixture data have to be included for identifying pure component parameters and that, in fact, no dipole-related parameter at all has to be regressed for small molecules.

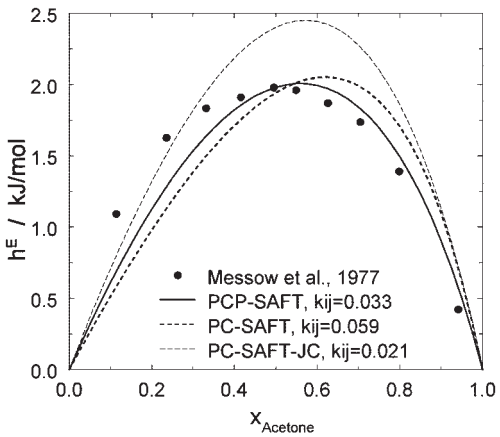

Figure 17. Excess enthalpy of mixing for the acetone–*n*-decane mixture at $T = 25°C$.

Comparison of PCP-SAFT, PC-SAFT, and PC-SAFT-Jog–Chapman calculations to experimental data.[51] Binary interaction parameters k_{ij} were adjusted to VLE data (see Figure 16).

The dipole expression of Saager and Fischer can be applied with the PC-SAFT EOS by applying the conversion relations Eqs. 5 and 6. This scheme, however, is applicable only for molecules with segment numbers of ≤ 2, so that acetone for example with segment numbers of approximately 2.5 is excluded. An alternative mixing scheme was applied by Gross and Sadowski[20] (without detailing the equations, however) and later published by Dominik et al.[54] A representative calculation result for mixtures is given in Figure 14. The Saager–Fischer PC-SAFT model (PC-SAFT-SF) describes mixture equilibria very similar to the nonpolar PC-SAFT model, but with the advantage of a lower value of k_{ij}. Compared to an earlier implementation,[54] the PC-SAFT-SF model can further be refined, by multiplying Eq. 10 of Dominik et al.[54] with $m_i/1.5222$, where 1.5222 is the segment number equivalent to an elongation of $L^* = 0.505$. This modification closely mimics the dependence of density on the elongation L^* as considered in the 2CLJ framework.[35] According to our experience, however, neither this refinement nor the consideration of a one-fluid mixing scheme as proposed by Müller et al.[55] leads to a general improved description of mixtures, when compared to the nonpolar PC-SAFT EOS (although lower k_{ij} values are required). In this light the results obtained from PCP-SAFT can be appreciated as providing systematic improvements in the de-

scription of pure components and mixtures of real substances.

Conclusions

The equation of state contribution for dipolar interactions developed in this work is suitable for dipolar molecules in the two-center Lennard–Jones framework as well as for tangent-sphere molecules (like that realized in the SAFT family) and is therefore applicable with different equations of state. The EOS contribution is based on a third-order perturbation theory, where model constants were adjusted to molecular simulation data for the vapor–liquid equilibrium of two-center Lennard–Jones plus pointdipole molecules, covering molecular elongations from $L^* = 0$ (spherical Stockmayer fluid) to $L^* = 1$ (dipolar Lennard–Jones dimer fluid). Although the temperature ranges covered by the considered simulation data are limited to the critical points, the Joule–Thomson inversion points were also well predicted by the model for higher temperatures. The model was compared to simulation data of polar mixtures and very good results were found for vapor–liquid as well as for liquid–liquid systems. When applied to real substances with the PC-SAFT EOS a clear improvement in the description of pure component behavior was achieved without introducing an additional pure component parameter. Rather, dipole moments from the literature can be used directly. The EOS was applied to the phase equilibrium of mixtures and revealed an improved representation of the experimental data, whereas the required binary interaction parameter was decreased at the same time, indicating an enhanced predictive capability of the model.

Literature Cited

1. Gross J. An equation of state contribution for polar components: Quadrupolar molecules. *AIChE J.* 2005;51:2556-2568.
2. Stell G, Rasaiah JC, Narang H. Thermodynamic perturbation theory for simple polar fluids, I. *Mol Phys.* 1972;23:393-406.
3. Stell G, Rasaiah JC, Narang H. Thermodynamic perturbation theory for simple polar fluids, II. *Mol Phys.* 1974;27:1393-1414.
4. Rushbrooke GS, Stell G, Høye JS. Theory of polar liquids. I. Dipolar hard spheres. *Mol Phys.* 1973;26:1199-1215.
5. Henderson D, Blum L, Tani A. Equation of state of ionic fluids. In: Chao KC, Robinson RL, eds. *Equations of State. Theories and Applications*. ACS Symposium Series 300. Washington, DC: American Chemical Society; 1986:281-296.
6. Gubbins KE, Twu CH. Thermodynamics of polyatomic fluid mixtures—I. Theory. *Chem Eng Sci.* 1978;33:863-878.
7. Twu CH, Gubbins KE. Thermodynamics of polyatomic fluid mixtures—II. Polar, quadrupolar and octopolar molecules. *Chem Eng Sci.* 1978;33:879-887.
8. Vimalchand P, Donohue MD, Celmins I. Thermodynamics of multipolar molecules: The perturbed anisotropic-chain theory. In: Chao KC, Robinson RL, eds. *Equations of State. Theories and Applications*. ACS Symposium Series 300. Washington, DC: American Chemical Society; 1986:297-313.
9. Cottermann RL, Schwarz BJ, Prausnitz JM. Molecular thermodynamics for fluids at low and high densities. Part I: Pure fluids containing small or large molecules. *AIChE J.* 1986;32:1787-1798.
10. Cottermann RL, Prausnitz JM. Molecular thermodynamics for fluids at low and high densities. Part II: Phase equilibria for mixtures containing components with large differences in molecular size or potential energy. *AIChE J.* 1986;32:1799-1812.
11. Chapman WG, Jackson G, Gubbins KE. Phase equilibria of associating fluids. Chain molecules with multiple bonding sites. *Mol Phys.* 1988;65:1057-1079.
12. Wertheim MS. Fluids with highly directional attractive forces: I. Statistical thermodynamics. *J Stat Phys.* 1984;35:19-34.
13. Wertheim MS. Fluids with highly directional attractive forces: II. Thermodynamic perturbation theory and integral equations. *J Stat Phys.* 1984;35:35-47.
14. Wertheim MS. Fluids with highly directional attractive forces: III. Multiple attraction sites. *J Stat Phys.* 1986;42:459-476.
15. Wertheim MS. Fluids with highly directional attractive forces: IV. Equilibrium polymerization. *J Stat Phys.* 1986;42:477-492.
16. Kraska T, Gubbins KE. Phase equilibria calculations with a modified SAFT equation of state. 1. Pure alcanes, alkanols, and water. *Ind Eng Chem Res.* 1996;35:4727-4737.
17. Jog PK, Chapman WG. Application of Wertheim's thermodynamic perturbation theory to dipolar hard sphere chains. *Mol Phys.* 1999;97:307-319.
18. Gross J, Sadowski G. Application of perturbation theory to a hard-chain reference fluid: An equation of state for square-well chains. *Fluid Phase Equilib.* 2000;168:183-199.
19. Gross J, Sadowski G. Perturbed-chain SAFT: An equation of state based on a perturbation theory for chain molecules. *Ind Eng Chem Res.* 2001;40:1244-1260.
20. Gross J, Sadowski G. Perturbed-chain SAFT: Development of a new equation of state for simple, associating, multipolar and polymeric compounds. In: Brunner G, ed. *Supercritical Fluids as Solvents and Reaction Media*. Amsterdam, The Netherlands: Elsevier Science; 2004.
21. Saager B, Fischer J. Construction and application of physically based equations of state. Part II. The dipolar and quadrupolar contributions to the Helmholtz energy. *Fluid Phase Equilib.* 1992;72:67-88.
22. Tumakaka F, Sadowski G. Application of the perturbed-Chain SAFT equation of state to polar systems. *Fluid Phase Equilib.* 2004;217:233-239.
23. Boublik T. Perturbation theory for pure quadrupolar hard Gaussian overlap fluids. *Mol Phys.* 1990;69:497-505.
24. Boublik T. Perturbation theory of polar nonspherical molecule fluids. *Mol Phys.* 1992;76:327-336.
25. Lupkowski M, Monson PA. Structure and thermodynamics of polar interaction site fluids. *Mol Phys.* 1988:63;875-890.
26. Lupkowski M, Monson PA. Phase diagrams of interaction site fluids. II. Dipolar diatomics. *Mol Phys.* 1989:67;53-66.
27. McGuigan DB, Lupkowski M, Paquet DM, Monson PA. Phase diagrams of interaction site fluids. I. Homonuclear 12-6 diatomics. *Mol Phys.* 1989:67;33-52.
28. Dubey GS, O'Shea SF, Monson PA. Vapor–liquid equilibria for the two center Lennard–Jones diatomics and dipolar diatomics. *Mol Phys.* 1993;80:997-1007.
29. Saager B, Fischer J, Neumann M. Reaction field simulations of monatomic and diatomic dipolar fluids. *Mol Simul.* 1991;6:27-49.
30. Müller A, Winkelmann J, Fischer J. Backone family of equations of state: 1. Nonpolar and polar pure fluids. *AIChE J.* 1996;42:1116-1126.
31. Weingerl U, Wendland M, Fischer J, Müller A, Winkelmann J. Backone family of equations of state: 2. Nonpolar and polar fluid mixtures. *AIChE J.* 2001;47:705-717.
32. Calero S, Wendland M, Fischer J. Description of alternative refrigerants with BACKONE equations. *Fluid Phase Equilib.* 1998;152:1-22.
33. Stoll J, Vrabec J, Hasse H. Comprehensive study of the vapour–liquid equilibria of the pure two-centre Lennard–Jones plus pointdipole fluid. *Fluid Phase Equilib.* 2003;209:29-53.
34. Gray CG, Gubbins KE. *Theory of Molecular Fluids*. Vol. I. Oxford, UK: Clarendon Press; 1984.
35. Lisal M, Aim K, Mecke M, Fischer J. Revised equation of state for two-center Lennard–Jones fluids. *Int J Thermophys.* 2004;25:159-173.
36. Johnson K, Müller EA, Gubbins KE. Equation of state for Lennard–Jones chains. *J Phys Chem.* 1994;98:6413-6419.
37. Stoll J, Vrabec J, Hasse H, Fischer J. Comprehensive study of the vapour–liquid equilibria of the pure two-centre Lennard–Jones plus pointquadrupole fluid. *Fluid Phase Equilib.* 2001;179:339-362.
38. Jog PK, Sauer S, Blaesing J, Chapman WG. Application of dipolar chain theory to the phase behavior of polar fluids and mixtures. *Ind Eng Chem Res.* 2001;40:4641-4648.
39. Walsh JM, Jin G, Donohue MD. Thermodynamics of short-chain polar compounds. *Fluid Phase Equilib.* 1991;65:209-237.
40. (a) Vega C, Saager B, Fischer J. Molecular dynamics studies for the new refrigerant R152a with simple model potentials. *Mol Phys.* 1989;68:1079-1093; (b) Vega C, McBride C, Menduina C. The second virial coefficient of the dipolar two center Lennard–Jones model. *Phys Chem Chem Phys.* 2002;4:3000-3007.

41. Vrabec J, Kumar Kedia G, Hasse H. Prediction of Joule–Thomson inversion curves for pure fluids and one mixture by molecular simulation. *Cryogenics.* 2005;45:253-258.
42. Stoll J. *Molecular Models for the Prediction of Thermophysical Properties of Pure Fluids and Mixtures*. PhD Dissertation. Stuttgart, Germany: Universität Stuttgart; 2004.
43. Gao GT, Wang W, Zeng XC. Gibbs ensemble simulation of HCFC/HFC mixtures by effective Stockmayer potential. *Fluid Phase Equilib.* 1999;158/160:69-78.
44. De Leeuw SW, Smit B, Williams CP. Molecular dynamics studies of polar/nonpolar fluid mixtures. I. Mixtures of Lennard–Jones and Stockmayer fluids. *J Chem Phys.* 1990;93:2704-2714.
45. Müller A, Winkelmann J, Fischer J. Simulation studies on mixtures of dipolar and nonpolar linear molecules. I. Liquid/liquid phase separation. *Fluid Phase Equilib.* 1994;99:35-47.
46. Lide DR. *CRC Handbook of Chemistry and Physics. Table* "*Dipole Moments*. " Cleveland, OH: CRC Press; 2004.
47. Huang SH, Radosz M. Equation of state for small, large, polydisperse, and associating molecules. *Ind Eng Chem Res.* 1990;29:2284-2294.
48. Ohgaki K, Sand F, Katayama T. Isothermal vapor–liquid equilibrium data for binary systems containing ethane at high pressures. *J Chem Eng Data.* 1976;21:55-58.
49. Matvienko VG, YarymAgaev NL. Liquid–vapor-equilibrium in the system *n*-butane–acetone. *Russ J Appl Chem.* 1994;67:145-147.
50. Campbell SW, Wilsak RA, Thodos G. Isothermal vapor–liquid equilibrium measurements for the *n*-pentane–acetone system at 372.7, 397.7, and 422.6 K. *J Chem Eng Data.* 1986;31:424-430.
51. Messow U, Doyé U, Kuntzsch S, Kuchenbecker D. Thermodynamische Untersuchungen an Lösungsmittel/n-Paraffin Systemen. V. Die Systeme Aceton/n-Decan, Aceton/n-Dodecan, Aceton/n-Tetradecan und Aceton/n-Hexadecan. *Z Phys Chem.* 1977;258:90-96.
52. Nissema A, Karvo M. Thermodynamic properties of binary and ternary systems. Part V. Vapor pressures and thermodynamic excess functions of toluene + dimethyl sulphoxide mixtures. *Finn Chem Lett.* 1977;8:222-226.
53. Lin ST, Sandler SI. Multipole corrections to account for structure and proximity effects in group contribution methods: Octanol–water partition coefficients. *J Phys Chem.* 2000;104:7099-7105.
54. Dominik A, Chapman WG, Kleiner M, Sadowski G. Modeling of polar systems with the perturbed-chain SAFT (PC-SAFT) equation of state. Investigation of the performance of two polar terms. *Ind Eng Chem Res.* 2005;44:6928–6938.
55. Müller A, Winkelmann J, Fischer J. Simulation studies on mixtures of dipolar and nonpolar linear molecules. II. A mixing rule for the dipolar contribution to the Helmholtz energy. *Fluid Phase Equilib.* 1996;120:107-119.

Manuscript received May 19, 2005, and revision received July 20, 2005.